Development of new tip-loss corrections based on vortex theory and vortex methods

Branlard, Emmanuel Simon Pierre; Gaunaa, Mac

Published in:
Journal of Physics: Conference Series (Online)

Link to article, DOI:
10.1088/1742-6596/555/1/012012

Publication date:
2014

Document Version
Publisher's PDF, also known as Version of record

Development of new tip-loss corrections based on vortex theory and vortex methods

2014 J. Phys.: Conf. Ser. 555 012012

(http://iopscience.iop.org/1742-6596/555/1/012012)

Development of new tip-loss corrections based on vortex theory and vortex methods

Emmanuel Branlard - Mac Gaunaa
DTU Wind Energy , 4000 Roskilde, Denmark
E-mail: ebra@dtu.dk

Abstract. A new analytical formulation of the tip-loss factor is established based on helical vortex filament solutions. The derived tip-loss factor can be applied to wind-turbines, propellers or other rotary wings. Similar numerical formulations are used to assess the influence of wake expansion on tip-losses. Theodorsen's theory is successfully applied for the first time to assess the wake expansion behind a wind turbine. The tip-loss corrections obtained are compared with the ones from Prandtl and Glauert and implemented within a new Blade Element Momentum(BEM) code. Wake expansion is seen to reduce tip-losses and have a greater influence than wake distortion.

1. Introduction

Tip-losses commonly refer to kinematic and/or dynamic differences between a two-dimensional and a three dimensional configuration of a lifting device. The main source of these differences for a wing of finite span or for a rotating device of finite number of blades is the circulation flow driven by the pressure equalization which arises at the tip of the lifting device. Prandtl used vortex theory analysis to assess the proportion of these losses for both a wing [1] and a propeller blade [2] at the beginning of the 20^{th} century. The latter study was introduced as a correction factor to be applied to Betz's optimal circulation [3] extending the applicability of Betz's result from an infinite to a finite number of blades. Prandtl's simplified model considers the axi-symmetric wake flow about a series of semi-infinite rigid lines. Glauert [4] suggested a modification to Prandtl's tip-loss factor for a convenient numerical implementation and it is his model which has been retained to this day in most BEM codes.

Recently, a free wake lifting-line code (see e.g. [5], [6]) was used to derive tip-loss corrections accounting for wake expansion, roll-up and distortion, and applicable to a wide range of operation conditions contrary to Prandtl's tip-loss factor. Following this approach, the present study will make use of analytical vortex results to derive a new analytical tip-loss factor, derive various numerical counterparts and study the influence of wake expansion on tip-losses. The structure of this article is as follow. First, the original definition of the tip-losss factor is presented together with different modern definitions. Then, the vortex-based tools required for the new analytical and numerical tip-loss factors derived in this study are briefly described. The presentation of the methodology follows and the last section of this document is dedicated to results and discussions.

2. Tip-loss factors within vortex theory

As a discussion following the work of Betz [2], Prandtl derived an approximate correction to establish the optimal circulation of rotors with finite number of blades. A detailed derivation and generalization of Prandtl's tip-loss factor can be found in [7]. Prandtl introduced a factor to compute the circulation on the blade Γ_B as function of the optimal circulation of Betz Γ_∞. One intepretation of Prandtl's tip-loss factor is the ratio between these two circulations, namely:

$$F_\Gamma = \frac{\Gamma_B}{\Gamma_\infty} \tag{1}$$

This definition also allows the computation of Goldstein's tip-loss factor by using Goldstein's circulation solution [8] for Γ_B. This method is described in [7]. Prandtl's tip-loss factor can also be interpreted as a correction term applied to induction factors. The definition of tip-losses in terms of induction factors is elaborated below. Let us assume that the entire flow field is known for a given rotor with B blades at a given operating condition. Such flow field can be obtained with vortex methods or other computational fluid dynamics methods. It is also assumed that the flow field is known in the case of a very large number of blades. The configuration with very large number of blades, considered as an infinite number of blades, does not present any tip-loss and the rotor is seen as an actuator disk. A tip-loss factor can be derived as the ratio between the induced velocity found on a blade for the case of an infinite number of blades to the equivalent value found for a finite number of blades. Such ratio can be computed for both the axial and tangential velocities or similarly for their corresponding induction factors a and a'. This approach leads to the definition of the two following tip-loss factors:

$$F_a = \frac{a_\infty}{a_B} \quad , \qquad F_{a'} = \frac{a'_\infty}{a'_B} \tag{2}$$

The ∞-subscript in the above refers to the case of an infinite number of blades. This definition will be referred to as the natural definition of the tip-loss factor. The tip-loss factor represents in some BEM codes implementations the proportion in which the axial induction at the blades differs from the momentum theory value. The momentum value is sometimes seen as a average value over an annulus of the rotor. From this perspective another definition of tip-losses can be established as e.g. in [9]. This tip-loss factor will be referred to as the planar tip-loss factor and will be defined as the ratio between the average induction in a circular annulus to the one on the blade, namely:

$$F_{\langle a \rangle} = \frac{\langle a \rangle_\theta}{a_B} \quad , \qquad F_{\langle a' \rangle} = \frac{\langle a' \rangle_\theta}{a'_B} \tag{3}$$

In the above, the brackets refer to the azimuthal average in an annulus defined between the radii r and $r + dr$:

$$\langle \bullet \rangle_\theta = \frac{1}{2\pi} \int_0^{2\pi} \bullet \, d\theta \tag{4}$$

3. Vortex-based tools used for the study of the tip-loss factor

The different vortex theory tools used in this study are briefly presented in the following. Vortex-theory reasoning and analytical expressions are presented in the first and second paragraphs. These results will simplify the induced-velocity computations required by the expressions of the tip-loss factors. The key aspects of the implemented wake models are discussed in the last paragraph.

3.1. Results from vortex filament analysis

Several results from vortex filaments analysis are developed in the following in light of their application to the study of tip-losses.

First result In the case of an axi-symmetric wake and by assuming that the wake shape is the same for any number of blades, the natural tip-loss factor and the planar tip-loss factors are the same. These assumptions are satisfied in particular in the case of a non-expanding wake consisting in different trailed helical filaments. This result can easily be proven analytically but is similarly obtained by a simple reasoning illustrated by figure 1. Let us consider the case of one blade with bound circulation Γ and the corresponding case of B blades, which by conservation of circulation will each have the bound circulation Γ/B. The intensities of the two systems of trailed vorticity will also have a factor $1/B$ between them. Now let us consider an elementary trailed vortex filament belonging to the wake of the single bladed case and the B corresponding elements from the B bladed case which are actually obtained from the former by B successive rotations of angle $2\pi/B$ around the rotor axis. It is easily seen that the sum of the contributions of the B azimuthal elements with intensity scaled by $1/B$ on one control point on the blade is equal to the average contribution from one element with full intensity on B different azimuthal positions. This demonstration is easily extended to an infinite number of blades and azimuthal control points by using integrals instead of summations and limits instead of direct circulation intensity.

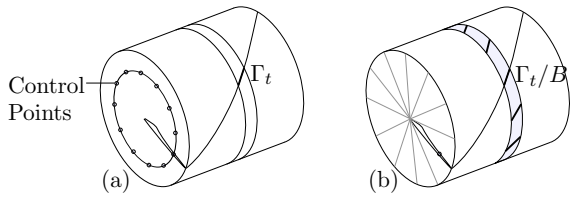

Figure 1. Planar and natural tip-loss factor computed respectively using a large number of: control points (a) or blades (b).

Second result By considering an infinite helical filament, any plane perpendicular to it would slice the helix in two semi-infinite helices. The induced velocities generated by the two semi-helices are the same on the radial line supporting the helix in the slicing plane but also symmetric with respect to that line. As a result of this the induced velocities on the radial line supporting the semi-infinite helix are half the one obtained with an infinite helix.

Third result The azimuthal average of the induced velocities on a plane perpendicular to the helix axis and from which a semi-infinite helix is emitted is half the value found for an infinite helix. This is found from an analysis similar to the previous paragraph due to the symmetry of the induced velocities with respect to the radial line supporting the helix. This result can also be derived more formally by considering for instance two elementary elements at equal distance to the slicing plane and use the parity of the induced velocity function in the longitudinal coordinate and its 2π-periodicity in the azimuthal coordinate without actually making explicit the induced velocity function.

3.2. Analytical expressions for helical vortex filaments

The analytical tip-loss factor developed in section 4 of this paper will make use of analytical approximation of the velocity field induced by a semi-infinite helical vortex filament. It will be assumed below that a regular semi-infinite helical vortex is trailed from each B blade of a rotor from the tip at position $r = r_0$. The blades are considered as lifting-lines. The helices from all blades are regular, they do not expand, they have the same pitch $h = 2\pi l$ and circulation intensity Γ_t. The helices surround the z axis from $z = 0$ to infinity. A sign parameter is

introduced with value $s = -1$ for left-handed helix(usual wind turbines) and $s = 1$ for right-handed helix(usual propellers). From the second result of section 3.1, the induced velocities at the lifting line are computed as half the velocities induced by an infinite helix. Radial induced velocities are null on the lifting line and are not used in this study. The tangential induction is directly related to the axial induction with $u_\theta = u_0 - s u_z l/r$, where $u_0 = B\Gamma_t/4\pi r$ for a semi-infinite helix or twice this value for an infinite helix. The potential corresponding to a system of B equally-spaced infinite helical filaments was derived by Kawada in 1936 [10]. Lerbs [11], derived an approximation of Kawada's expression. Later, in 1957, Wrench [12] added a correction term to improve the accuracy of this approximation. The axial velocity induced by B semi-infinite helical filaments on the lifting line is obtained from Wrench formula as:

$$s\,u_z(r) = \frac{B\Gamma_t}{4\pi l}\left\{\begin{matrix}1\\0\end{matrix}\right\} + \frac{B\Gamma_t}{4\pi l}\left(\frac{l^2+r_0^2}{l^2+r^2}\right)^{\frac{1}{4}}\left[\frac{\pm 1}{e^{\mp B\xi}-1} + \frac{1}{B}C_{1z}\log\left(1+\frac{1}{e^{\mp B\xi}-1}\right)\right] \tag{5}$$

with

$$C_{1z} = \frac{l}{24}\left[\frac{9r_0^2+2l^2}{(l^2+r_0^2)^{\frac{3}{2}}} + \frac{3r^2-2l^2}{(l^2+r^2)^{\frac{3}{2}}}\right], \qquad e^{\xi} = \frac{r}{r_0}\frac{\left(l+\sqrt{l^2+r_0^2}\right)}{\left(l+\sqrt{l^2+r^2}\right)}\frac{\exp\left(\sqrt{l^2+r^2}/l\right)}{\exp\left(\sqrt{l^2+r_0^2}/l\right)} \tag{6}$$

In (5) the upper value of the bracket should be used for radial positions such that $r < r_0$, and the sign notation $\pm$ or $\mp$ follow the same stacking layout than the bracket notation. The attention is drawn on the required factor $1/l$ in (6) if comparison is to be done with other references. It can be shown that (5) is equal to the summation over B helical filaments of the approximate solution from Okulov [13] using properties of the roots of unity and simple polynomial algebra.

3.3. Analytical and numerical wake models

The velocity field at the rotor plane is entirely determined by the wake geometry in the context of potential theory of a symmetric rotor. As a result of this, different tip-loss factors will be obtained from different vortex wake models. Different prescribed and free wake models were implemented in this study to investigate these differences. The reader is referred to [7] and [5] for a description of the free wake lifting-line code. This section will focus on key aspects of the prescribed wake models used. The simplest and fastest prescribed wake model implemented makes use of the analytical expression presented in section 3.2 and allow the calculation of the natural and planar tip-loss factors analytically. The wake consists of a series of semi-infinite helical filaments trailed along the blade. The helix pitches are computed using the velocity triangle immediately downstream of the blade as illustrated in figure 2 and with the following expression:

$$h(r) \equiv 2\pi r \tan\epsilon(r) = \frac{2\pi U_0(1-a(r))}{\Omega(1+2a'(r))} \tag{7}$$

The pitch angle is determined solely by the velocity triangle if the rotor is operating at low-loading and without wake expansion. Under these assumptions the pitch of a trailed filament can be assumed to be constant along the wake and equation (7) can be used. This relation will be assumed to hold in practice for different loading conditions. This approximation is required for relative comparisons between the case of expanding and non-expanding wakes. A numerical analog to the theoretical helical wake model has been implemented but being more computationally expensive, its analytical counterpart will always be preferred. This numerical analog though can be slightly modified to account for wake expansion. In a very simple fashion, an expansion factor as function of the downstream location can be applied to

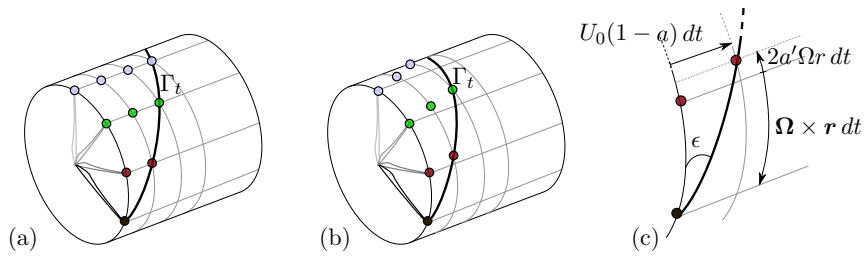

Figure 2. Trailed velocity path and relation to induced velocities for a one-bladed rotor. Four Lagrangian particles are plotted, each represented by one color. The particles passed through the tip of the blade at four different times. The line joining these particles at a given time is the trailed vorticity line. (a) Without tangential induction - (b) With tangential induction - (c) Helix angle related to induced velocities.

the trailed vortex filament. Different expansion factors have been used including the theoretical one from Theodorsen [14] defined as:

$$\frac{R_w(\overline{z})}{R} = 1 - s\frac{c_t}{\kappa}\frac{\bar{l}^3}{4}\int_X^{\overline{z}/\bar{l}}\int_\theta^\infty\int_0^1 \frac{G(x,\bar{l},B)}{B}\sum_{b=1}^{B} y_1(\theta,x,2\pi b/B)dxd\theta d\theta \tag{8}$$

with $X = 0$ for wind turbines and $X = \infty$ for propellers and the function y_1 being defined as:

$$y_1(x,\theta,\tau) = \frac{\left(1-2x^2+\bar{l}^2\theta^2+x\cos(\tau+\theta)\right)}{\left(1+x^2+\bar{l}^2\theta^2-2x\cos(\tau+\theta)\right)^{\frac{5}{2}}}\left[\theta\cos(\tau+\theta)-\sin(\tau+\theta)\right] \tag{9}$$

The above equations are entirely determined by the knowledge of the dimensionless torsional parameter $\bar{l} = h/2\pi R$ and the thrust coefficient in the far wake c_t. The Goldstein factor is defined as $G = B\Gamma/hw$, with w being the "rigid-wake" relative velocity, and

$$\kappa = 2\int_0^1 G(x,\bar{l},B)x\,dx \tag{10}$$

Illustration of different expansions obtained using Theodorsen's theory are plotted in figure 3 for a same value of $\overline{w} = w/U_0$. The determination of the far-wake parameters as function of the near-wake $\{\lambda, C_T\}$ is done using an iterative procedure along the same line as the methodology presented in [15] and [16]. Another prescribed wake model used is the one from Gaunaa[17] which also requires numerical computation. It includes wake expansion and distortion with varying pitches along the wake and different convection velocities and rotational velocities of the vortex elements. This model was established based on the results from free wake computations.

4. Analysis of tip-loss using vortex methods and vortex theory

The available tools described in section 3.3 consist in: different numerical prescribed wake code, an analytical prescribed wake formulation and a free wake code. The natural and planar tip-loss factor defined in section 1 can be computed with each of these methods. If no analytical expression is available, the case with "very large" number of blades is computed with 60 times more blades than the finite number of blade case. The equivalence between planar and natural tip-loss factors within the validity range from the first result of section 3.1 has been verified as

a validation case. For the analytical method, the natural tip-loss factor has a direct analytical expression given by equation (11). This method is hence convenient to compute tip-losses without wake expansion. For numerical methods it is the opposite: the planar tip-loss factor is the fastest to be retrieved. The case with very-large number of blades is indeed computationally expensive. Given the context of this study, the equivalence between the tip-loss factors is always satisfied and the definition giving the fastest computational time will be chosen for each case.

The formula of the new analytical tip-loss factor derived in this study is made explicit below. This tip-loss factor is more easily computed using the natural definition but the planar definition could be used as well thanks to the third result from section 3.1. At a given radial position, the tip-loss is the ratio between the total induced velocity from the helical vortex filaments of the infinitely-bladed case to the induced velocity of the finite case:

$$F(r) = \frac{\lim\limits_{B_l \to \infty} \int_0^R u_{z,B_l}\left(r, r_0, h(r_0), \Gamma_t(r_0)/B_l\right) dr_0}{\int_0^R u_{z,B}\left(r, r_0, h(r_0), \Gamma_t(r_0)\right) dr_0} \tag{11}$$

where $u_{z,B}$ is the sum of induced velocities from B helical filaments emitted at radial position r_0 as given by (5). For each radial position, the proper circulation Γ_t and helical pitch $h = 2\pi l$ as defined by (7) should be used. In practice the flow angle is known at finite positions and the integral is replaced by a summation. The limit is removed from vortex cylinder theory results:

$$u_{z,\infty} = \lim_{B_l \to \infty} u_{z,B_l} = \frac{\Gamma_t}{2h} \begin{Bmatrix} 1 \\ 0 \end{Bmatrix} \tag{12}$$

using the same brackets convention as in section 3.2.

In order to compare the different methods, two different circulation shapes will be prescribed to the various codes for different operating conditions. The two circulation curves are plotted on the right of figure 3. The first one corresponds to a case of high loading towards the root of the blade. The curve is obtained with the parameters $\{x_0 = 0.3, x_2 = 0.5, y_3 = 0.5, t_0 = 0.3\}$, corresponding to the coordinates of the Bézier points according to the parametrization developed in earlier work by the authors [5]. The second circulation shape corresponds to the Goldstein circulation obtained for far-wake values $\{1/\bar{l} = 9.1, \overline{w} = 0.45\}$. Simulations were run for the six

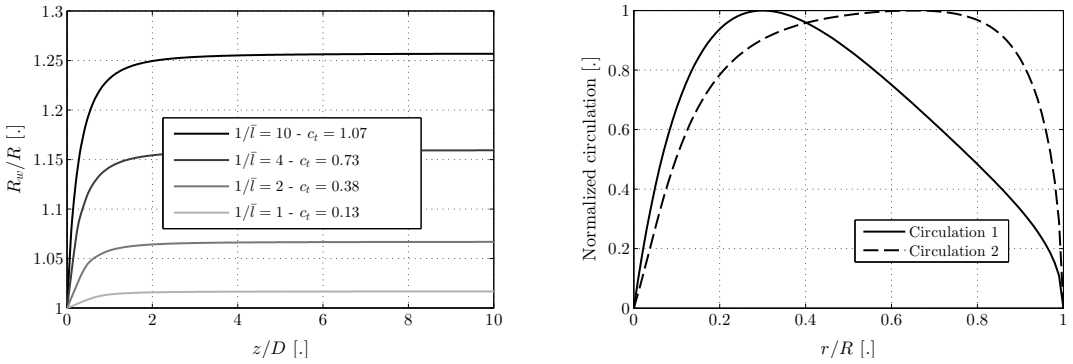

Figure 3. (left) Wake Expansion factor computed using Theodorsen's theory for different far wake pitch and $\overline{w} = 0.4$ - (right) Circulation shapes used for the study of tip-losses.

sets of values $\{\lambda, C_T\}$ found in table 1. For each set, the amplitude of the circulation shape that gives the design thrust coefficient is computed using a BEM code embedded in an optimization routine. The circulation with the right amplitude is then prescribed to the different codes. To

quantify the differences between the different tip-loss factors found by the different methods a parameter referred to as the lost area, and noted A_F, is introduced. The lost area is simply the difference between the area of the unit-square and the area below the tip-loss curve when expressed in terms of dimensionless radius. A large loss area signifies large tip-losses and hence a large difference between the inductions obtained with finite and infinite number of blades.

5. Results and discussions

The different codes were run for the two circulation curves and the six sets of rotor parameters presented in section 4. For each case, the tip-loss factor and the lost area were computed. Results are reported in table 1. For simplicity only four codes are used for comparison. In the table, the line entitled "BEM" refers to the tip-loss factor obtained in Glauert's sense within a BEM code with prescribed circulation. The line entitled "Helix" corresponds to results from the new analytical tip-loss factor of equation (11). The line "Helix+Exp." stands for the simple prescribed wake model that uses Theodorsen's theory to compute the wake expansion. Last, the line "Free Wake" designs the tip-loss results obtained by the free wake lifting line vortex code. As an illustration, tip-loss factors obtained with the two analytical methods are shown in figure 4 (left).

Table 1. Lost Area A_F in percentage of the unit-square area computed for the six sets of operational parameters and the two circulation shapes.

	Circulation 1						Circulation 2					
λ	7.0	7.0	7.0	3.0	7.0	12.0	7.0	7.0	7.0	3.0	7.0	12.0
$\mathbf{C_T}$	0.2	0.5	0.7	0.6	0.6	0.6	0.2	0.5	0.7	0.6	0.6	0.6
BEM	6.2	5.8	5.5	11.1	5.6	3.5	6.1	5.4	4.8	10.2	5.1	3.1
Helix	5.9	6.0	6.2	9.7	6.1	4.3	7.3	6.7	6.2	11.2	6.4	4.3
Helix+Exp.	5.3	4.3	3.8	6.0	4.0	2.8	6.9	5.6	4.8	9.5	5.2	3.4
Free Wake	3.6	3.1	2.6	7.1	2.8	1.7	5.4	4.5	3.8	8.2	4.2	2.4

From table 1 several trends can be outlined. The most general trend is that all the methods give the expected result that tip-losses are reduced with increasing tip-speed ratio and increasing C_T. This is observed with decreasing values of A_F for increasing values of λ or C_T. This trend can be explained by the increased proximity of the vortex sheets occurring with the increase of these parameters. Indeed, using 1D momentum theory, (7) and the assumption of infinite tip-speed ratio ($a' = 0$) one obtains the following measure for the proximity of the sheets $h = \frac{\pi R}{\lambda}\left[1 + \sqrt{1 - C_T}\right]$ [5].

Comparisons between BEM code and free-wake code results follow the conclusions from a previous study [5]: the tip-loss factors obtained with Glauert's formulation often have a larger lost area than the one obtained by the free-wake code. Yet, since the nature of the two codes is different the comparison can be quite abstruse. On the contrary comparisons amongst vortex codes are justified and offer great potential. By looking at the three last lines of table 1, it is observed that the lost area is always reduced when going from the simplest model to the more advanced free-wake model suggesting that both expansion and distortion of the wake tend to decrease the proportion of tip-losses. The sole effect of expansion on the tip-loss function is illustrated on the right of figure 4. In both cases illustrated the prescribed wake models with expansion show a lower lost area. Gaunaa's advanced prescribed wake model gave similar tip-loss functions than the simpler helical wake model with Theodorsen's wake expansion, showing coherence between the expansion models and suggesting that the expansion model is more influential than the distortion model for the study of tip-losses.

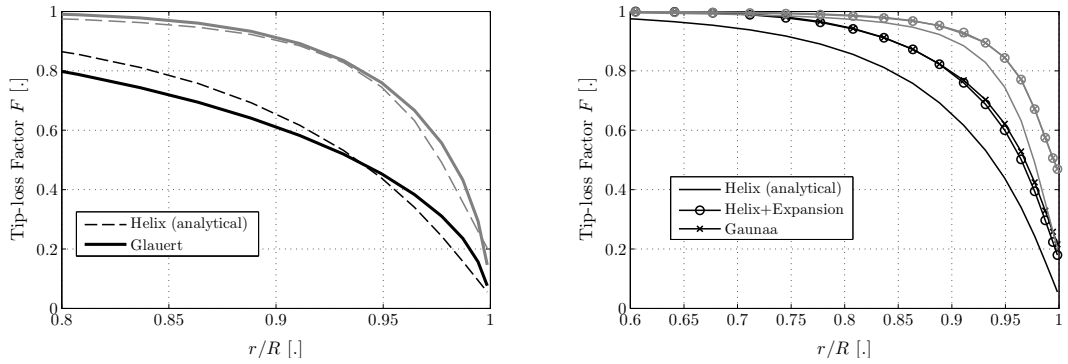

Figure 4. Tip-loss factors for different tip-speed ratios. (left) Comparison of the two analytical tip-loss factors - (right) Effect of expansion. The darker curve corresponds to $\lambda = 3$ and the lighter one to $\lambda = 12$, while $C_T = 0.6$ and Circulation 1 is used in both cases..

6. Conclusion

Distinctions and clarifications between different possible definitions of tip-losses have been presented. By superposition of semi-infinite helical filaments whose pitches depend on the velocity triangle after the rotor, a tip-loss factor can be computed using analytical formulae. This new analytical tip-loss factor is easily implemented in a BEM code. The method is physically more advanced than the one originally presented by Prandtl. The two analytical methods give coherent results. The expansion factor from Theodorsen has been successfully applied to wind energy for the first time. The influence of wake expansion on the tip-loss factor has been studied with vortex methods. It was seen that the wake expansion has a greater influence on the tip-losses than the wake distortion. Despite the simplicity of the prescribed wake model used, it was possible to capture the fact that wake expansion reduces tip-loss. This result was confirmed by using free-wake simulations. Development of advanced numerical methods and accurate measurements of flow in the rotor plane will help reveal which of the methods assesses best the phenomenon of tip-losses.

References

[1] Prandtl L 1921 *Applications of modern hydrodynamics to aeronautics* (NACA report No. 116)
[2] Prandtl L 1919 *Göttinger Klassiker der Strömungsmechanik Bd. 3* p89–92 (in German)
[3] Betz A 1919 *Göttinger Klassiker der Strömungsmechanik Bd. 3* p68–88 (in German)
[4] Glauert H 1935 *Airplane propellers, Division L* w.f. durand (ed) ed vol 4 (Julius Springer)
[5] Branlard E, Dixon K and Gaunaa M 2013 *IET Renewable Power Generation* **7** 311–320 ISSN 1752-1416
[6] Branlard E, Dixon K and Gaunaa M 2012 *Proceedings* (EWEA - The European Wind Energy Association)
[7] Branlard E 2011 *Wind turbine tip-loss corrections: Review, implementation and investigation of new models* Master's thesis Risø-DTU, Siemens Energy Inc. (available at DTU's library)
[8] Goldstein S 1929 On the vortex theory of screw propellers Tech. rep. St. John's College, Cambridge
[9] Shen W Z, Mikkelsen R, Sørensen J N and Bak C 2005 *Wind Energy* **8** p457–475
[10] Kawada S 1936 *Journal of Aeronautical Sciences* **3**
[11] Lerbs H 1952 *Transactions of the Society of Naval Architects and Marine Engineer* **60** 73–117
[12] Wrench J 1957 *Reprint od Applied Mathematics Laboratory Tecnical Report 13*
[13] Okulov V L 1995 *Russian Journal of Engineering Thermophysics* **5** 63–75
[14] Theodorsen T 1948 *Theory of propellers* (New York: McGraw-Hill Book Company)
[15] Okulov V and Sørensen J 2008 *Doklady Physics* **53** p337–342
[16] Wald Q 2006 *Progress in Aerospace Science* **42**
[17] Gaunaa M, Sørensen N and Døssing M 2011 *AIAA Aerospace Sciences Meeting* **543**